

Influence of the sintering time and pressing force of the pellets on the morphology of the superconducting phases in BSCCO system

M. C. BUNESCU

METAV-S.A., Bucharest, P.O. Box 18/3, Romania

G. ALDICA, F. VASILIU

Institute of Physics and Technology of Materials, Bucharest, MG-7, Romania

P. NITA, E. VASILE

METAV-S.A., Bucharest, P.O. Box 18/3, Romania

The influence of the sintering time and pressing force on the pellets on the occurrence and morphology of the superconducting phases in BSCCO system were studied. Scanning electron microscopy, X-ray microanalysis and X-ray diffraction were used to identify the phases and their morphologies. The 2223 crystals had a plate-like morphology and 2212, a polyhedral-like one. The optimum parameters in order to obtain a majority of 2223 phase were identified: i.e. a longer sintering time and medium pressing force. © 2000 Kluwer Academic Publishers

1. Introduction

It is well known that a great number of technological parameters influence the quality and properties of the superconducting ceramic Bi-Sr-Ca-Cu-O (BSCCO): the starting composition [1–3], the heat treatment and routes [4–6], the intermediate grindings and other mechanical treatments [7–9], etc.

V. Sima *et al.* [8] have compared the influence of combined mechanical and heat treatment on $\text{Bi}_2\text{Sr}_2\text{Ca}_2\text{Cu}_3\text{O}_{10+\gamma}$ (2223) phase formation. They concluded that the mechanical treatment increases the density of the lattice defects which act as nucleation centres for 2223 phase. Thus, they have got better results on mechanically treated samples than on the samples which suffered only heat treatment.

Our study is concerned with the influence of the sintering time and pressing force of the pellets on the occurrence and morphology of the superconducting phases in the BSCCO system.

2. Experimental

Three sets of pellets with the nominal composition $\text{Bi}_{1.7}\text{Pb}_{0.3}\text{Sr}_2\text{Ca}_2\text{Cu}_3\text{O}_x$ were prepared by sintering appropriate amounts of precursor $\text{Sr}_2\text{Ca}_2\text{Cu}_3\text{O}_7$, Bi_2O_3 and PbO , at 860°C , for 20 hs (Set A), 70 hs (Set B), and 260 hs (Set C). For each set the pellets ($10 \times 3 \times 3 \text{ mm}^3$) were pressed with three different forces: 8, 16 and 24 kbar.

A SEM-515 scanning electron microscope equipped with an energy dispersive X-ray spectrometer (EDS), and a HZG-4A X-ray diffractometer were used to analyse the occurrence and morphology of the superconducting phases of the pellets. The electron microscopy

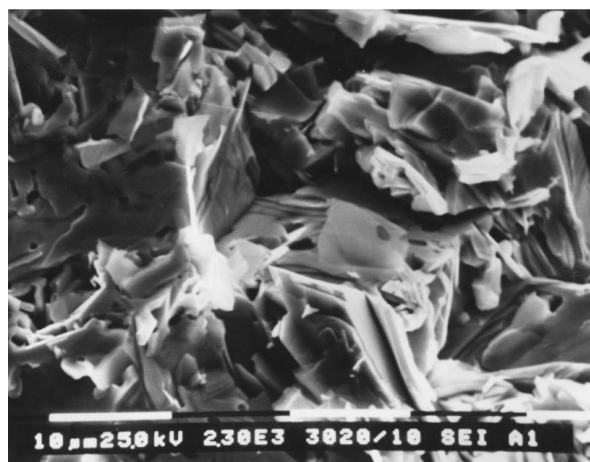
analyses were performed on fresh fracture surfaces to have a real image about the dimensions and morphology of the crystals. The X-ray diffraction analyses were performed on the powder obtained by crushing each pellet, using $\text{Cu K}\alpha$ characteristic radiation ($\lambda = 1.5418\text{\AA}$). The temperature dependence of the electrical resistance was measured between 77 and 300 K using the standard four probe method.

3. Results and discussions

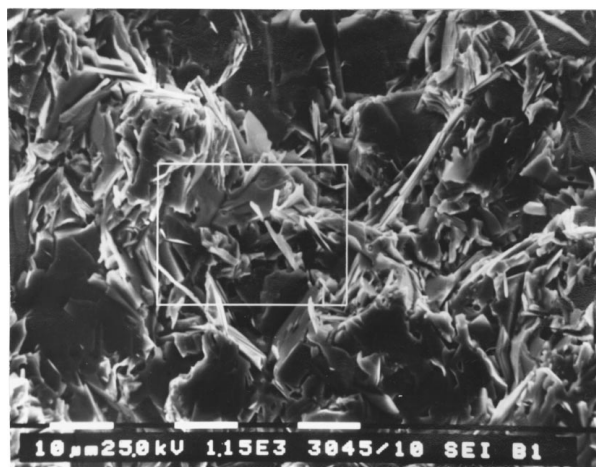
The scanning electron microscope (SEM) images presented in Figs 1, 2 and 3 show the morphology of the crystals in Set A, Set B and Set C samples, each of them pressed with 8, 16 and 24 kbar. Plate-like and polyhedral crystals have been observed. The polyhedral crystals have had a particular morphology: polygonal pores on the external surfaces (marked by arrows in Fig. 1) can be observed, suggesting that the crystal was formed by the intergrowth of many plate-like crystals on different directions.

The longer sintering time seems to favour the occurrence of plate-like morphology. Thus, in the samples from Set C a higher density of plates could be observed, while in Set A a greater number of those particular shape polyhedra have been observed. Another modification due to the variation of the sintering time was the average dimension of the crystals which increased with the sintering time from $10 \mu\text{m}$ (Set A) to $30 \mu\text{m}$ (Set C).

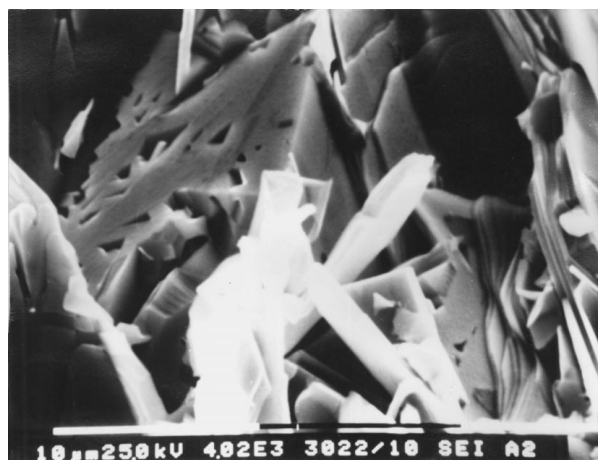
The micro-porosity of the material was not influenced by the different pressing forces applied. No improvement of the compactness of the material (studied from this scanning electron microscopy point of



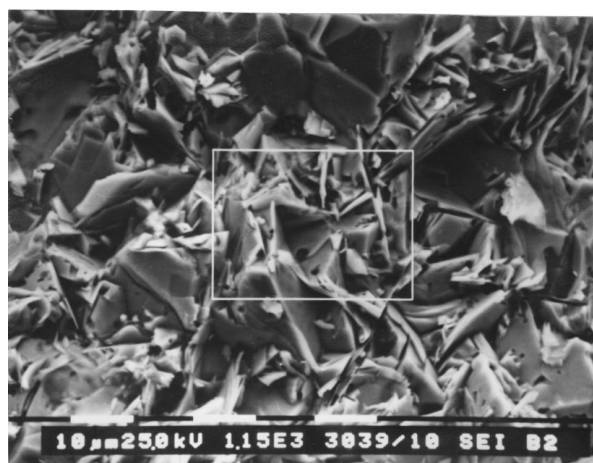
(a)



(a)



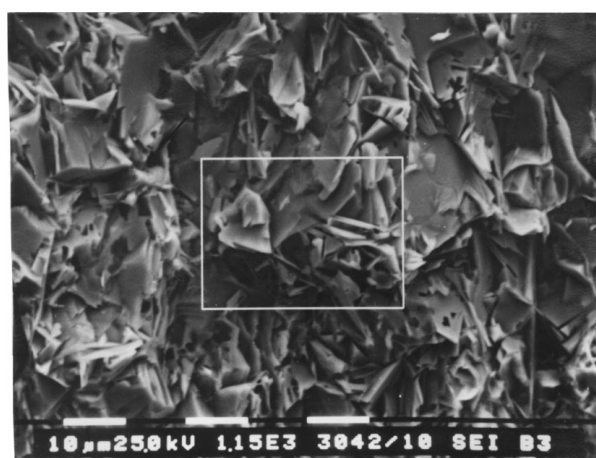
(b)



(b)



(c)



(c)

Figure 1 SEM image of the pellets in set A: a) 8 kbar; b) 16 kbar; c) 24 kbar.

Figure 2 SEM image of the pellets in set B: a) 8 kbar; b) 16 kbar; c) 24 kbar.

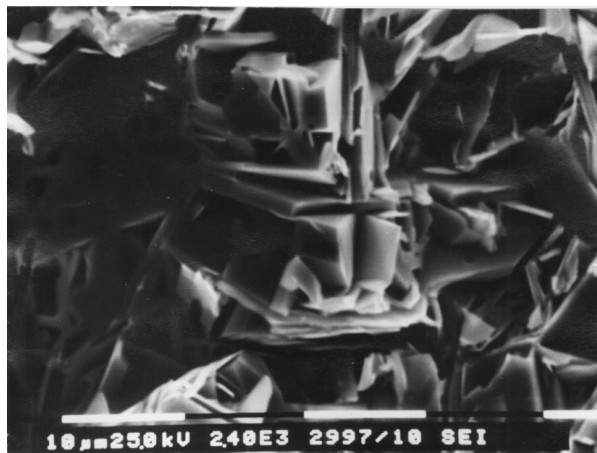
view) have been observed when higher pressing forces were applied. Anyway, the variation of this parameter did not seem to have an observable influence on the morphology, dimensions and composition of the crystals.

The results of the local chemical composition analyses performed by EDS are presented in Table I. The plate-like crystals have had a stoichiometric ratio close to the 2223 superconducting phase, while the polyhedral ones have had both 2212 and 2223 compositions. As compared to a stoichiometric nominal composition

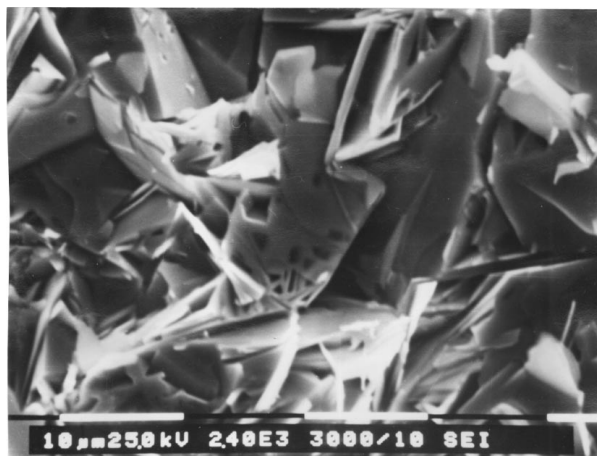
(relative to Cu content), it must be noted that the high T_c phase (2223) had a Bi excess, whereas the low T_c phase (2212) exhibited a (Sr, Ca) deficiency and, sometimes, a lower Bi content. A few crystals were complex Sr-Ca-Cu oxides. Thus, the occurrence of the high T_c superconducting phase 2223 has increased with the sintering time, result which is in agreement with the data already reported [5, 6, 10]. No influence of the pressing force on the occurrence of the 2223 phase have been noticed by these SEM and EDS analyses. The X-ray diffraction patterns obtained on crushed powder from



(a)



(b)



(c)

Figure 3 SEM image of the pellets in set C: a) 8 kbar; b) 16 kbar; c) 24 kbar.

each pellet are presented in Figs 4, 5 and 6. A few qualitative observations could be made:

- both 2212 (L) and 2223 (H) phases have been identified in all samples;
- the influence of the pressing force of the pellets could be appreciated if the ratio between the (115) peaks of the two phases ($2\theta_H = 26.25$ deg and $2\theta_L = 27.52$ deg) have been analysed; it is obvious that the

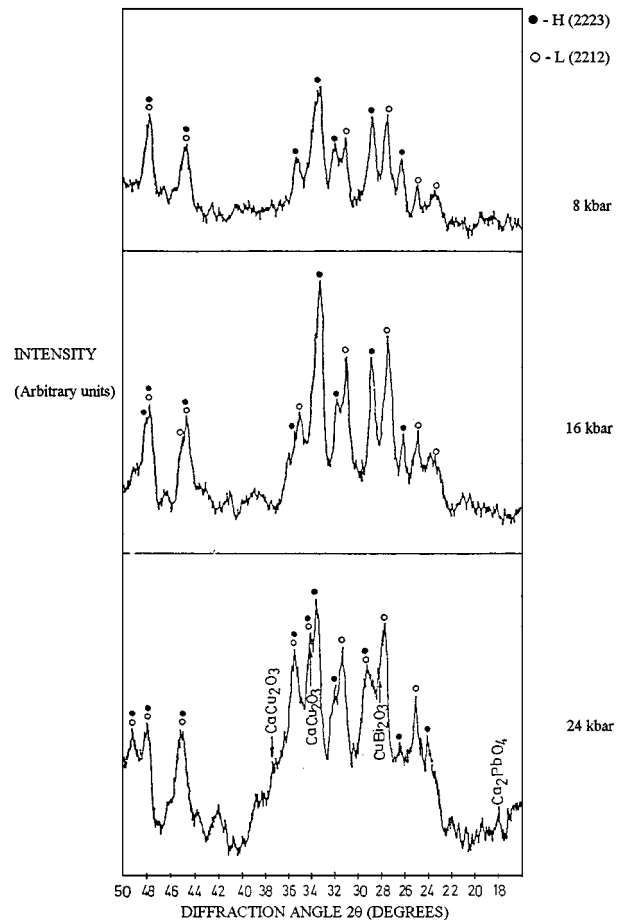


Figure 4 X-ray diffraction pattern for Set A samples.

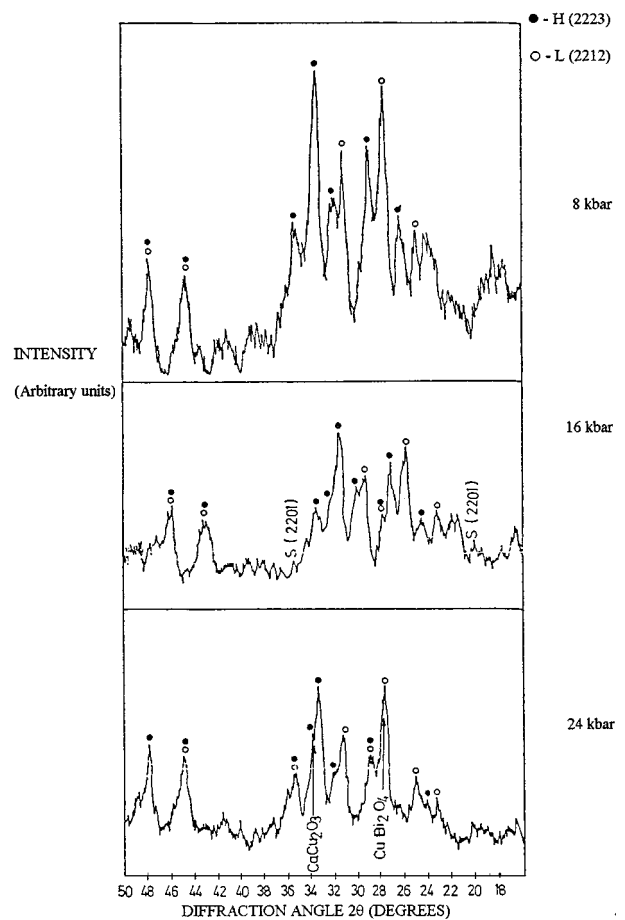


Figure 5 X-ray diffraction pattern for Set B samples.

TABLE I X-ray microanalysis (EDS) results

Crystal type	Chemical composition (at%)					(Bi+Pb):Sr:Ca:Cu ratios
	Bi	Pb	Sr	Ca	Cu	
Set A						
Plate-like	11.59	2.48	11.21	8.95	17.42	(2+0.4):1.9:1.5:3
Plate-like	11.26	2.56	11.20	10.04	16.48	(2+0.4):2:1.8:3
Polyhedral	12.43	3.38	10.89	7.63	17.09	(1.5+0.4):1.3:0.9:2
Polyhedral	1.47	0.21	8.84	8.81	30.93	Residual
Set B						
Plate-like	12.14	2.23	11.42	9.23	16.89	(2.1+0.4):2:1.6:3
Plate-like	10.96	2.35	10.25	10.51	17.49	(1.9+0.4):1.8:1.8:3
Polyhedral	10.90	2.15	10.14	11.20	17.26	(1.3+0.3):1.2:1.3:2
Polyhedral	13.06	2.26	11.22	8.99	16.61	(1.5+0.3)1.3:1.1:2
Polyhedral	1.05	0.13	9.42	7.27	32.34	Residual
Set C						
Plate-like	10.73	2.21	10.78	10.42	17.45	(1.8+0.4):1.8:1.8:3
Polyhedral	11.60	2.12	11.81	7.42	18.89	(1.8+0.3):1.9:1.2:3
Polyhedral	13.83	2.23	12.57	6.41	17.68	(2.3+0.4):2.1:1.1:3
Polyhedral	10.98	1.95	12.10	9.24	17.50	(1.9+0.3):2.1:1.6:3

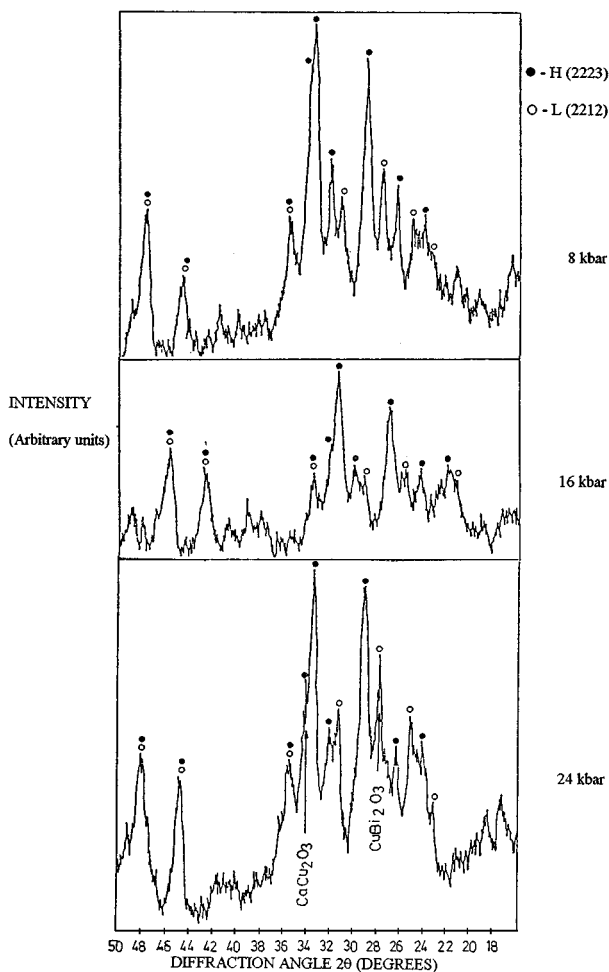


Figure 6 X-ray diffraction pattern for Set C samples.

intensity of the H(115) peak increased with the pressing force at each sintering time; the most favourable ratio of these two peaks (majority of the H phase) has been obtained for the sample in Set C pressed with 16 kbar;

– the peak at $2\theta = 21.67$ deg could be attributed to the semiconducting phase of the system—2201 (S) whose existence is very probable in this system;

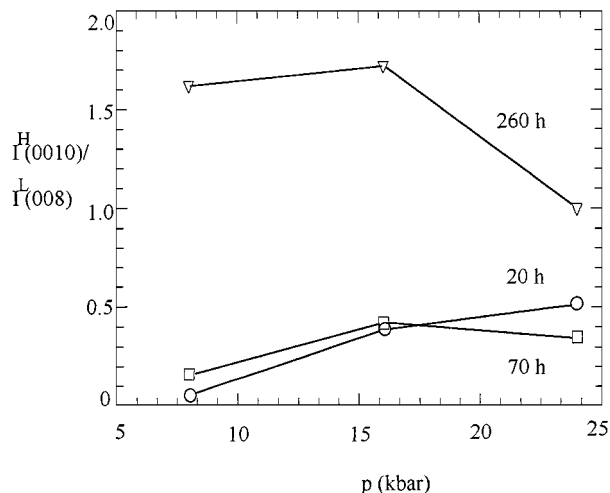


Figure 7 Intensity ratio of (0010)H/(008)L vs pressing force.

– the Sr-Ca-Cu oxides observed by the EDS analyses could be complex oxides type CuBi_2O_4 , CaCu_2O_3 , Sr_2CuO_3 , Ca_2PbO_4 whose main diffraction peaks overlap the peaks of the superconducting phases of the system.

The plots in Fig. 7 show the ratio 2223/2212 measured as the ratio of the intensities (0010)H/(008)L. For short sintering times the amount of 2223 phase increased uniformly with the pressure applied. For longer sintering times an optimum pressure (16 kbar) for the growth and formation of 2223 phase could be observed. Higher pressing forces resulted in worse results. For short sintering times the pressures applied have had a beneficial effect, indicating a straight dependence of the compacticity of the material on the transformation reaction from 2212 + liquid phase + secondary phases to 2223. For longer sintering times the absence of a liquid phase has prevented the reaction; some of the most dense groups of 2212 phase have not reacted with the Ca-Sr-Cu-O type phases to form the 2223 phase.

The results of the density measurement are presented in Table II and Fig. 8. The density has decreased with the

TABLE II Variation of the apparent density (g/cm^3) with the sintering time and pressing force

Sample/sintering time	Pressing force (kbar)		
	8	16	24
Set A (20 hs)	5.71	5.90	5.91
Set B (70 hs)	5.63	5.53	5.70
Set C (260 hs)	5.38	5.50	5.32

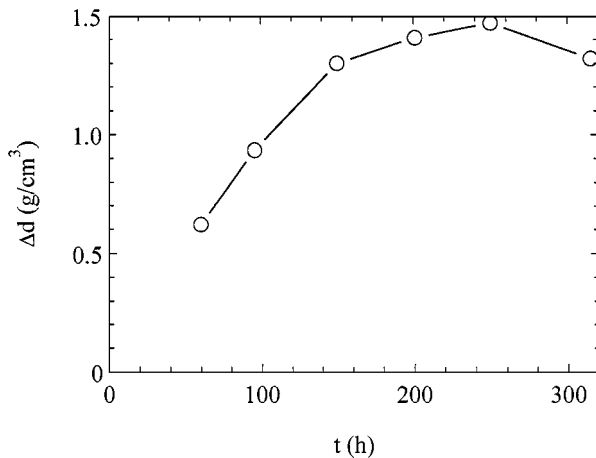


Figure 8 Apparent density ($\Delta d = d - d_0$, where d and d_0 are the densities after and before the sintering) vs sintering time.

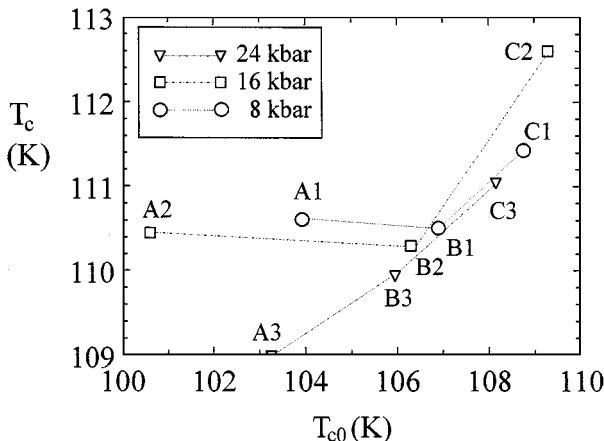


Figure 9 Correlation between T_c and T_{c0} for the three sets of samples.

sintering time. The variation of the pressing force has had a minor influence on the transformation processes of 2212 to 2223. These results are consistent with the above observations.

The temperature dependence of the electrical resistance has evidenced a usual behaviour of the samples. All curves have had a "metallic" aspect between 180 and 300 K, and a transition temperature over 100 K. The influence of the pressing force and sintering time on T_c and T_{c0} is presented in Fig. 9. A different behaviour of the pellets pressed with 24 kbar could be observed. The difference between T_c and T_{c0} has decreased when the sintering time has increased (Set C). The best values

has been obtained for the sample in Set C pressed with 16 kbar, indicating that plate-like is the most favourable morphology of the 2223 phase and its growth mechanisms were optimum for a medium pressing force.

4. Conclusions

The dominant morphology of the crystals observed was plate-like and polyhedral. The polyhedral crystals had a particular morphology, suggesting that they were formed by the intergrowth of many plate-like crystals on different directions. The average dimension of the crystals increased with the sintering time from 10 μm (Set A) to 30 μm (Set C). The plate-like crystals have had a stoichiometric ratio close to the 2223 superconducting phase (usually with a Bi excess) and the polyhedral ones have had both 2212 (Sr and Ca deficient) and 2223 compositions. The longer sintering time has favoured the occurrence of plate-like morphology of the 2223 phase.

For short sintering times the pressure applied has had a beneficial effect on the growth mechanism of 2223 phase, indicating a straight dependence of the compactness of the material on the transformation reaction from 2212 to 2223. For longer sintering times an optimum pressure (16 kbar) for the growth and formation of 2223 phase could be observed. The absence of a liquid phase due to more dense groups of 2212 phase has prevented the reaction between Ca-Sr-Cu-O type phases and 2212 to form 2223.

The best values for T_c and T_{c0} has been obtained for the sample in Set C pressed with 16 kbar, indicating that plate-like is the most favourable morphology of the 2223 phase and its growth mechanisms were optimum for a medium pressing force.

References

1. Q. WU, Z. FU, A. ZANG, J. HUANG, D. TANG, P. YAO, S. CHU, S. YI, X. RONG, A. ZHANG and X. CHENG, *J. Appl. Phys.* **71** (1992) 2772.
2. T. G. HOLESINGER, D. J. MILLER, L. S. CHUMBLEY, M. J. KRAMER and K. W. DENNIS, *Physica C* **202** (1992) 109.
3. S. H. KIM, Y. Y. KIM, S. H. LEE and K. H. KIM, *ibid.* **196** (1992) 27.
4. H. K. LEE, K. PARK and D. H. HA, *J. Appl. Phys.* **70** (1991) 2764.
5. D. PANDEY, A. K. SINGH and A. P. SINGH, *Physica C* **204** (1992) 179.
6. A. MAQSOOD, M. MAQSOOD, M. S. AWAN and N. AMIN, *J. Mat. Sci.* **26** (1991) 4893.
7. V. SESHU BAI, S. RAVI, T. RAJASEKHARAN and R. GOPALAN, *J. Appl. Phys.* **70** (1991) 4378.
8. V. SIMA, K. KNIZEK, J. CHAVAL, E. POLLERT, P. SVOBODA and P. VASEK, *Physica C* **203** (1992) 59.
9. P. NITA, F. VASILIU, F. CONSTANTINESCU, G. ALDICA and C. BUNESCU, *Rom. J. Phys.* **42**(9-10) (1997) 725.
10. R. HARADA, O. YOSHINARI and K. TANAKA, *Jap. J. Appl. Phys.* **31** (1992) 2420.

Received 9 September 1997

and accepted 30 September 1999